Substrate and Substrate Analog Binding to Endothelial Nitric Oxide Synthase: Electron Paramagnetic Resonance as an Isoform-Specific Probe of the Binding Mode of Substrate Analogs†

John C. Salerno,‡ Pavel Martásek,§ Robert F. Williams,§ and Bettie Sue S. Masters*,§

Biology Department, Rensselaer Polytechnic Institute, Troy, New York 12180, and Department of Biochemistry, The University of Texas Health Science Center at San Antonio, 7703 Floyd Curl Drive, San Antonio, Texas 78284-7760

Received December 6, 1996; Revised Manuscript Received July 21, 1997⊗

ABSTRACT: The binding of arginine analogs to endothelial nitric oxide synthase (eNOS, NOSIII) perturbs the environment of the high-spin ferriheme in a highly ligand-specific manner. Using electron paramagnetic resonance as a probe of heme ligation geometry, four categories of high-spin complex could be distinguished. These are analogous to the four classes of high-spin complexes, stabilized individually by the binding of L-arginine, *N*-hydroxy-L-arginine (NHA), *N*-methyl-L-arginine (NMA), and *N*-nitro-L-arginine (NNA), which we have previously reported for the other two isoforms. Each of these species is five-coordinate and retains the axial thiolate ligand but each differs in its ligation geometry. *N*-Methyl-L-arginine is a relatively poor inhibitor of eNOS, and the NMA complex of eNOS differs from the *N*-methyl-L-arginine complexes of inducible nitric oxide synthase (iNOS, NOSII) and neuronal nitric oxide synthase (nNOS, NOSI) in that it is of lower rhombicity. We previously showed that inducible nitric oxide synthase, which binds NNA less tightly than eNOS and nNOS, could not form the lower rhombicity NNA complex characteristic of nNOS. Endothelial nitric oxide synthase readily forms such lower rhombicity complexes, which correlates with the tight binding of NNA to this isoform. Arginine and tetrahydrobiopterin promote loss of the flavin free radical EPR signal, while arginine analog inhibitors stabilize the radical; this suggests that the residual flavin radicals can serve as a source of reducing equivalents for slow turnover in the absence of endogenous reductant.

Nitric oxide (NO)[1] has in the past decade proved to be an important signal molecule in numerous physiological processes (Ignarro *et al.*, 1987; Palmer *et al.*, 1987; Furchgott, 1988; Garthwaite *et al.*, 1988). NO is generated physiologically by nitric oxide synthases (NOS), a family of complex, modular enzymes. The endothelial and neuronal isoforms (eNOS and nNOS) are constitutive enzymes controlled by calcium/calmodulin (Abu-Soud & Stuehr, 1993). The inducible isoform, iNOS, is synthesized during the immune response (Hauschildt *et al.*, 1990; Knowles *et al.*, 1990; McCall *et al.*, 1989; Curran *et al.*, 1989) and is active at all physiological intracellular calcium levels.

Bredt and co-workers (1991) showed that the C-terminal half of nNOS is homologous to NADPH-cytochrome P450 reductase, an enzyme containing binding domains for FAD and FMN; the calmodulin binding site is located directly before the *N*-terminal of FMN binding domain in the sequence. All NOS isoforms contain heme (Mayer *et al.*, 1992; McMillan *et al.*, 1992; Stuehr & Ikeda-Saito, 1992; White *et al.*, 1992) and tetrahydrobiopterin (BH_4) (Mayer *et al.*, 1991), as well as FMN and FAD (Bredt *et al.*, 1991, 1992; Mayer *et al.*, 1991; Jaussens *et al.*, 1992; Lamas *et al.*, 1992; Lyons *et al.*, 1992; McMillan *et al.*, 1992; Xie *et al.*, 1992). The *N*-terminal region of NOS contains the catalytic domains, including the heme-binding region and the biopterin- and arginine-binding sites; the N- and C-terminal halves of the NOS isoforms have been independently expressed as hemoprotein and flavoprotein constructs (Ghosh & Stuehr, 1995; McMillan & Masters, 1995; Nishimura *et al.*, 1995; Chen *et al.*, 1996; Gachhui *et al.*, 1996; Masters *et al.*, 1996; Salerno *et al.*, 1996b).

Hibbs and co-workers (1987) established that L-arginine was the substrate of the NO synthesizing enzymes by showing that arginine analogs inhibited NO synthesis. NO is produced by NOS in two sequential monoxygenation reactions, forming citrulline as product and consuming 1.5 mol of NADPH/mol of NO formed (Iyengar *et al.*, 1987; Marletta *et al.*, 1988; Palmer *et al.*, 1988; Bromberg *et al.*, 1989). Recently, Campos *et al.* (1995) reported that substoichiometric levels of citrulline were formed from arginine in the absence of NADPH; the source of reducing equivalents was unclear.

We have shown recently, using electron paramagnetic resonance (EPR) spectroscopy, that the heme site of nNOS is perturbed by the binding of substrate (L-arginine), intermediate NHA, and arginine analog inhibitors, including thiocitrulline, homothiocitrulline, NMA, and NNA (Salerno *et al.*, 1995, 1996a); thiocitrulline had previously been shown to bind tightly to nNOS (Frey *et al.*, 1994). The ferriheme of nNOS holoenzyme was shown to exhibit EPR spectra characteristic of four high-spin states in response to the

† Supported by NIGMS Grant GM52419 and NHLBI Grant 30050 from the National Institutes of Health and Grant AQ-1192 from The Robert A. Welch Foundation (B.S.S.M.).

* To whom correspondence should be addressed.

‡ Rensslaer Polytechnic Institute.

§ The University of Texas Health Center at San Antonio.

⊗ Abstract published in *Advance ACS Abstracts,* September 15, 1997.

[1] Abbreviations: NO, nitric oxide; eNOS, endothelial nitric oxide synthase (NOSIII); iNOS, inducible nitric oxide synthase (NOSII); eNOS, neuronal nitric oxide synthase (NOSI); NHA, *N*-hydroxy-L-arginine; NMA, *N*-methyl-L-arginine; NNA, *N*-nitro-L-arginine; IEO, *N*-iminoethyl-L-ornithine; EPR, electron paramagnetic resonance; BH_4, tetrahydrobiopterin.

S0006-2960(96)03003-6 CCC: $14.00

binding of arginine site ligands. These states differ in ligation geometry and represent local conformations of the active site adopted in response to specific interactions of substituent groups within the heme pocket. Isoform specificity of arginine analog inhibitors is clinically important. To determine if another constitutive isoform, eNOS, exhibits similarities or differences to nNOS, we used EPR spectroscopy, and here we show that the response of the eNOS heme environment to arginine site ligands is similar to that of nNOS but that differences exist which appear to be highly relevant to the partial isoform specificity of arginine analog inhibitors.

METHODS

Materials. All chemicals used for purification were obtained from Sigma Chemical Co. NNA and BH_4 were from Research Biochemicals International (Natick, ME). L-Arginine, NHA, NMA, 7-nitroindazole, and *N*-iminoethyl-L-ornithine (IEO) were purchased from Alexis Corp. (San Diego, CA).

Expression and Purification of Bovine eNOS. Expression and purification of bovine eNOS were performed using procedures previously described (Martasek *et al.*, 1996). During the purification procedure, no BH_4 or L-arginine was added. Protein samples were frozen at −80 °C at 30 μM and used for sample preparation on the same day as EPR spectroscopy was performed. An additional purification step was included in cases of samples used for preparation of eNOS for crystallization attempts. We used a Superose 6 HR 10/30 column (Pharmacia Biotech AB, Uppsala, Sweden), flow rate 0.4 mL/min, buffer composition, 50 mM Tris-HCl, pH 7.5, 0.1 mM EDTA, 1 mM mercaptoethanol, 100 mM NaCl, 10% glycerol (v/v), detection in 400, 406, or 280 nm, respectively, using a LC-10AD liquid chromatograph and SPD-10AV UV−vis detector from Shimadzu. Column was calibrated using protein standards from Bio-Rad (Hercules, CA). Only the top fractions of a peak corresponding to eNOS dimer were collected and concentrated (A_{280}/A_{407} = 2.3−2.4; >95% purity based on PAGE/SDS gel).

Sample Preparation and Spectroscopy. Enzyme sample concentrations were determined on the basis of heme concentration and prepared for spectroscopy by addition of concentrated solutions of ligand to purified enzyme; in all cases, the volume change caused by ligand addition was <3%. Samples with ligand were incubated on ice for period of 15−20 min. If not stated differently, 10× M excess of ligands were added to eNOS preparations. Samples (0.25 mL) of eNOS at a final concentration of 15 μM (in the case of crystallization quality eNOS, 25 μM) were frozen for EPR measurements in quartz EPR tubes in a 6:1 isopentane−cyclohexane mixture cooled with liquid nitrogen and stored in liquid nitrogen. Spectra were recorded using a Bruker 300D EPR spectrometer and an Oxford liquid helium cryostat. Analysis of EPR spectra, including spin quantitation, was performed using standard methods as described in the previous communications (Salerno *et al.*, 1996a,b).

Unless otherwise noted, data presented here were obtained from samples which were not subjected to freeze−thaw cycles after initial sample preparation. The ligand complexes were all prepared with fresh enzyme; samples were never thawed and ligand was dialyzed away. Due to the difficulty in obtaining sufficient enzyme, a sample was sometimes thawed to compare the results of a short incubation with an overnight incubation. Two or three cycles of freezing and thawing has little effect on the EPR spectra of the enzyme; even after five cycles, the major effect is a slight loss of the native heme EPR signal. The EPR spectra of the enzyme are insensitive to glycerol concentration in the 10−20% range.

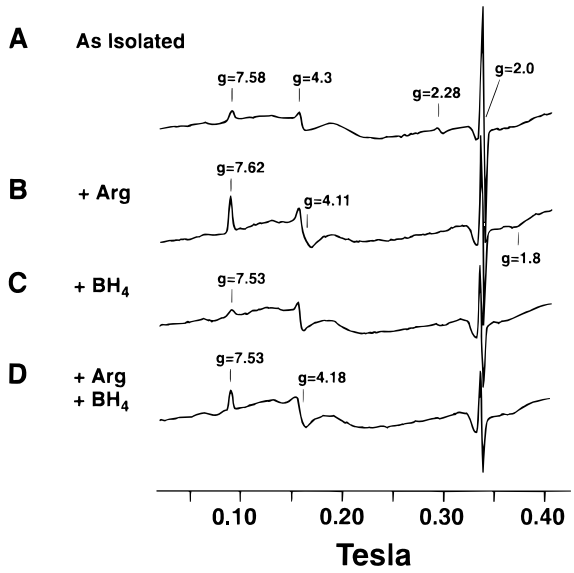

FIGURE 1: Effects of L-arginine and BH_4 on the electron paramagnetic resonance spectrum of eNOS ferriheme and flavosemiquinone radical. Line A, EPR spectrum of purified eNOS as isolated. Line B, spectrum after addition of L-arginine. Line C, spectrum after addition of BH_4. Line D, spectrum after addition of L-arginine and BH_4. Enzyme concentrations were 15 μM as measured by ferriheme CO binding spectra. Experimental conditions were sample temperature, 10 K; microwave power, 5 mW; modulation frequency, 100 kHz; modulation amplitude, 14.3 G; scan width, 0.4 T, center field, 0.21 T.

RESULTS

Electron Paramagnetic Resonance Spectrum of eNOS. The electron paramagnetic resonance spectrum of eNOS as isolated is shown in Figure 1, trace A. Features of the high-spin ferriheme are visible at $\mathbf{g}_x \approx 7.6$ and $\mathbf{g}_y \approx 4.0$; the latter feature is overlapped with the signal of the middle Kramers' doublet of high-spin, low-symmetry iron, present as a minor contaminant. The $\mathbf{g}_z$ feature, near $\mathbf{g} = 1.8$, is too weak to be identified with confidence. Only about 40% of the heme is in the high-spin ferric state. Low-spin ferriheme features are present at $\mathbf{g}_z = 2.42$, $\mathbf{g}_y = 2.28$, and $\mathbf{g}_x = 1.9$; under these conditions, they appear weak because of power saturation, but they are more intense at higher temperatures. Both the high- and low-spin states have an axial thiolate ligand, but the high-spin state is five-coordinate while the low-spin state has an oxygen ligand trans to the thiolate, probably from solvent water.

The sharp, intense signal at $\mathbf{g} = 2.0$ is contributed by flavosemiquinone, probably from FMNH. At this temperature, the radical signals are heavily saturated; spectra were also obtained under unsaturated conditions at higher temperature (spectra not shown). Changes in the radical signal observed in this communication are due to changes in semiquinone concentration rather than changes in relaxation rates. Weak, broad background signals are due to small amounts of liquid oxygen in the microwave cavity, and the broad signal near $\mathbf{g} = 2$ is a cavity contaminant.

Trace B shows the effect of L-arginine addition on the spectrum. L-Arginine binding drives the ferriheme almost totally high spin, and the features of the L-arginine complex are visible at $\mathbf{g}_z = 7.62$, $\mathbf{g}_y = 4.11$, and $\mathbf{g}_x = 1.8$. The low-spin signal has disappeared, while the intensity of the radical has slightly decreased in amplitude. Some of the changes in the high-spin ferriheme EPR spectrum are difficult to see with the broad field sweep shown but are readily observed with shorter sweeps (omitted here to save space) as in our previous communications.

Addition of BH_4 to the isolated enzyme produced the spectrum shown in Figure 1, trace C. The $\mathbf{g}_x$ feature of the high-spin ferriheme appears broadened and somewhat decreased in amplitude without a compensating increase in the low-spin features. The weak signals of minority states are difficult to quantitate accurately in the presence of overlapping species, but it appears that the increased line width and the increased amplitude at $\mathbf{g}_y$ are indicative of a slight increase in the fraction of the enzyme in the high-spin state. The most obvious effect of BH_4 addition is the decrease in the content of flavosemiquinone to approximately half its original value.

Trace D, Figure 1 shows the EPR spectrum of eNOS after addition of L-arginine and BH_4. Most of the heme has again been converted to a high-spin state, but the high-spin state produced has somewhat different characteristics from the corresponding species in the presence of L-arginine alone. The $\mathbf{g}_x$ feature ($\mathbf{g}_x = 7.53$) appears slightly broadened and shifted to higher field, while the $\mathbf{g}_y$ feature is shifted to lower field, indicative of a decrease in rhombicity.[2] The flavosemiquinone radical has only 40% of the intensity of the enzyme as isolated.

Overnight incubation with L-arginine and BH_4 produced a sample in which electron transfer was clearly as important as ligand binding in defining the final state. The heme is predominantly in a high-spin state which resembles the L-arginine complex. In this sample, there is no detectable flavosemiquinone radical. This implies the conversion of the odd-electron reductase domain states to even electron states, by either oxidation or reduction of the flavin cofactors. BH_4 is an obligatory two electron donor, so reduction of a monomer by BH_4 would not convert it from an odd-electron (paramagnetic) state to a even-electron state. Therefore, either electron transfer between reductase monomers or flavin-heme electron transfer is occurring, leading to slow turnover, ferroheme production, or some combination of the two.

Binding of L-Arginine Analogs to eNOS:NHA. We recently showed that binding of L-arginine, NHA (the obligatory intermediate), and arginine site ligands produced characteristic changes in the EPR spectra of nNOS ferriheme which depended on the nature of the substituents presented to the heme pocket (Salerno *et al.,* 1996a). The states produced with nNOS holoenzyme fell into four categories, which could be described as arginine-like, NHA-like, NMA-like, and NNA-like.

Figure 2, trace A, shows the EPR spectrum of eNOS plus *N*-hydroxy-L-arginine (NHA): NHA binding converts the

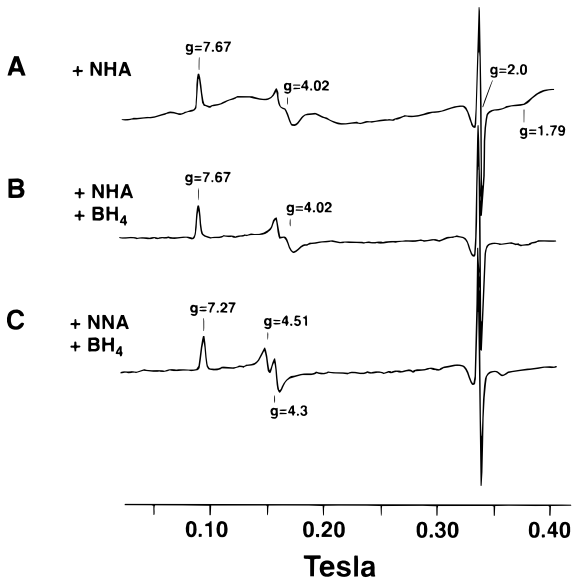

FIGURE 2: Effects on the eNOS ferriheme and flavosemiquinone electron paramagnetic resonance spectra of the binding of the intermediate, NHA, and the inhibitor NNA in the presence of BH_4. Line A, EPR spectrum of eNOS as isolated. Line B, spectrum after addition of NHA and BH_4. Line C, spectrum in the presence of NNA and BH_4. Conditions as in Figure 1.

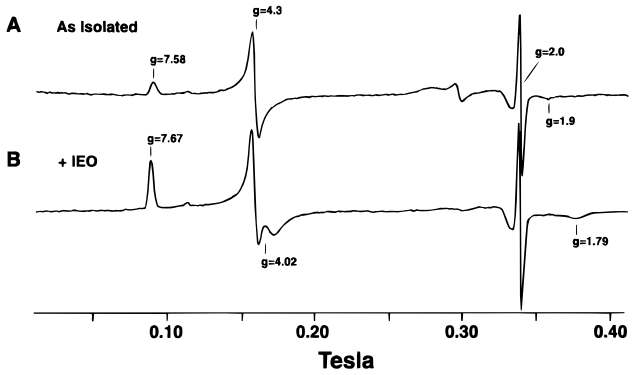

FIGURE 3: The effect of the inhibitor, IEO, on the eNOS ferriheme electron paramagnetic resonance spectra. Line A, EPR spectrum as isolated. Line B, Spectrum with IEO added. Conditions as in Figure 1.

eNOS ferriheme almost quantitatively to high spin, producing a single species. The **g** tensor of this species is similar to that of the nNOS NHA complex; $\mathbf{g}_x = 7.67$, $\mathbf{g}_y = 4.02$, and $\mathbf{g}_z = 1.79$. The rhombicity is significantly greater than that of either eNOS as isolated or the eNOS arginine complex and just slightly less than that of the NHA complexes of the other two isoforms.

The loss of the low-spin features ($\mathbf{g} = 2.42$ and $\mathbf{g} = 2.28$) in comparison to Figure 1A is obvious, but the decrease in the intensity of the flavosemiquinone signal at $\mathbf{g} = 2.0$ is much less pronounced than the results obtained (Figure 1) with L-arginine and BH_4. The apparent decrease in radical intensity caused by NHA is less than 10% and may not be significant. Overnight incubation at 4 °C after addition of BH_4 to the same sample produced no further effect (other than a subtle change in the lineshape of the high-spin ferriheme signal) as shown in the spectrum of trace B.

Binding of IEO to eNOS. *N*-Iminoornithine (IEO) forms an arginine-like high-spin complex with nNOS. The EPR spectrum (Figure 3) of the corresponding complex of eNOS is nearly identical to that of the eNOS NHA complex. This

[2] Rhombicity is defined in terms of the ratio of the rhombic and axial zero field splitting parameters *E* and *D*. These parameters reflect the separation of the iron d_{xz} and d_{yz} orbitals (E) and the separation of this pair from the dxy orbital. The rhombicity is a measure of the inequivalence of the in heme plane directions.

Table 1: High-Spin Complexes of eNOS Holoenzyme[a]

ligand	$\mathbf{g}_x$	$\mathbf{g}_y$	$\mathbf{g}_z$	*E*/*D*
group I: NMA-like				
N-methyl-L-arginine	7.73	3.95	1.78	.083
group II: NHA-like				
N-hydroxy-L-arginine	7.67	4.02	1.79	.081
N-iminoethyl ornithine	7.67	4.02	1.79	.081
group III: arginine-like				
as isolated	7.58	4.15	1.8	.075
L-arginine	7.62	4.11	1.8	.078
L-arginine + BH_4	7.53	4.18	1.8	.073
group IV: NNA-like				
N-nitro-L-arginine	7.27	4.51	1.88	.058
7-nitro indazole[b]	7.31	4.47	1.87	.061

[a] Entries show principal **g** values and zero field splitting parameters of the most important high-spin species observed in EPR experiments with eNOS. The species listed represent the majority of the ferriheme present unless otherwise noted. [b] A minority species is present which resembles those listed in group III.

is the only example we observed in which the eNOS complex of an arginine analog had a higher rhombicity than the corresponding nNOS complex. It is apparently the result of steric differences between the nNOS and eNOS sites which cause IEO to bind in an arginine-like mode in nNOS and an NHA-like mode in eNOS.

Binding of NNA. NNA is an inhibitor of all NOS isoforms, but has been reported to be much more effective as an inhibitor of eNOS and nNOS than as an inhibitor of iNOS. We recently reported that NNA binding by nNOS produced a strikingly less rhombic high-spin species with $\mathbf{g}_x \approx 7.3$ (Salerno *et al.*, 1996a). NNA binding by iNOS elicited a less pronounced decrease in rhombicity (Salerno, *et al.*, 1996b); the resulting species exhibited a $\mathbf{g}_x$ value of 7.5 and was only slightly less rhombic than the arginine complexes of the constitutive NOS isoforms. Trace C of Figure 2 shows the EPR spectrum of the eNOS NNA complex in the presence of BH_4. The $\mathbf{g}_x$ and $\mathbf{g}_y$ regions are dominated by a single high-spin species, with $\mathbf{g}_x = 7.27$ and $\mathbf{g}_y = 4.51$. This corresponds closely to the major high-spin species elicited by NNA binding to nNOS (Salerno *et al.*, 1996a).

NNA addition resulted in the loss of low-spin signals (Figure 2C relative to Figure 1A), but more significantly, the free radical signal of flavosemiquinone remained essentially undiminished compared to the enzyme as isolated (Figure 1, trace A). Since this sample was prepared by addition of NNA to an eNOS sample previously treated with BH_4, the result suggests that arginine analogs have the potential to reverse rather than merely protect against the BH_4-initiated decrease in radical observed in Figure 1.

7-Nitroindazole forms two high-spin complexes with nNOS, one of which resembles the NNA complex (Salerno *et al.*, 1996a) and the other of which is slightly lower in rhombicity than the arginine complex. Similar complexes are formed with eNOS; the NNA-like form is predominant (spectra not shown; Table 1).

Binding of NMA. While *N*-methyl-L-arginine (NMA) is an inhibitor of all NOS isoforms, it has been reported to be much more effective as an inhibitor of iNOS and nNOS (Reif & McCreedy, 1995) than of eNOS. It binds tightly but reversibly to the enzyme as isolated but, in the presence of NADPH, it can be metabolized to form an irreversible inhibitor−enzyme complex. NMA binding by eNOS resulted in almost complete conversion of ferriheme to a single high-spin state. The new high-spin species has $\mathbf{g}_x = 7.73$ and $\mathbf{g}_y = 3.95$. While this represents a significant increase in rhombicity relative to high-spin ferriheme in eNOS as isolated, the increase in rhombicity produced by NMA binding is significantly smaller than the increased rhombicity we previously observed upon NMA binding to nNOS or iNOS (Salerno, *et al.*, 1996 a,b).

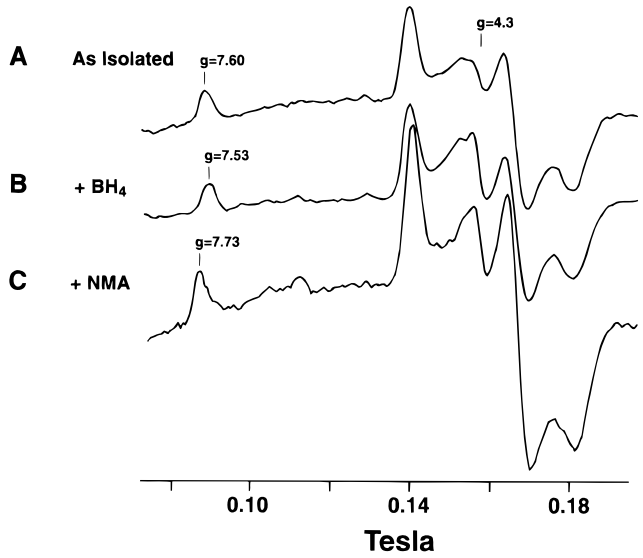

FIGURE 4: Electron paramagnetic resonance spectra of a cell lysate preparation from *E. coli* expressing eNOS. Line A, EPR spectrum of lysate as isolated. Line B, Spectrum of lysate with BH_4 added. Line C, Spectrum of lysate with NMA added. Conditions as in Figure 2.

Zero Field Splitting and Spin Quantitation. We recently reported (Salerno *et al.*, 1995) that the spin state equilibrium of nNOS showed no evidence of temperature dependence from 7 to 23 K. The temperature dependence of the high-spin ferriheme EPR spectra in nNOS could be accounted for in all cases by the Curie Law dependence arising from the population ratio within the lowest Kramer's doublet and an additional factor representing the Boltzmann equilibrium within the $S = {}^5/_2$ sextet, assuming the value of the axial zero field splitting parameter to be $D \approx 3.8$ cm^{-1}.

The general similarity of the EPR spectra of nNOS, iNOS, and eNOS ferrihemes suggest that the zero field splittings are similar for all three isoforms, although only the ratio *E*/*D* can be determined from peak positions. We do not yet have eNOS samples of sufficient concentration to examine a wide enough range of temperature to provide an accurate value of *D*. However, within the limits of signal quality, it appears that no significant temperature dependence of the spin state equilibrium exists between 7 and 20 K and that the temperature dependence of the high-spin EPR signals of all three NOS isoforms is similar, implying a value of $D \approx 4$ cm^{-1} in all cases.

EPR Spectra of eNOS in Crude Cell Lysates. Expression of eNOS in *Escherichia coli* was obtained at high enough levels to conduct spectroscopic experiments without purification. This is useful because it allows evaluation of the state of eNOS in a nearly *in situ* environment and because it allows the effects of arginine analog binding to be studied without purifying enzyme.

Figure 4, trace A, shows the EPR spectrum at 10 K in the $\mathbf{g}_x - \mathbf{g}_y$ region for high-spin ferriheme of cell lysate from *E. coli* expressing eNOS (eNOS lysate). The peak at $\mathbf{g} = 7.60$

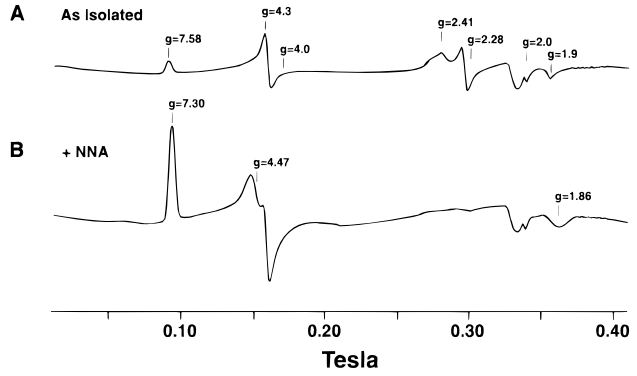

FIGURE 5: EPR spectrum of crystallization quality eNOS after incubation at 4 °C for three weeks. Line A, EPR spectrum of eNOS after incubation. Line B, EPR spectrum of eNOS sample after addition of NNA. Conditions as in Figure 1.

is the $\mathbf{g}_x$ feature of eNOS ferriheme. There is no significant interference from other cell components in this region. The position and form of the peak are indicative of the presence of an arginine complex of eNOS in the absence of BH_4 which is the majority species of the enzyme in the cells during expression. The complex of lines around $\mathbf{g} = 4.3$ is due to the expression of high levels of FeSOD. Spectra showing the range from 0.01 to 0.41 T (not shown) confirm that no significant levels of low-spin eNOS ferriheme are present. There is little interference from other cell components between 0.2 and 0.3 T, so observation of low-spin forms of eNOS ferriheme would be quite practicable.

Figure 4, trace B, shows the EPR spectrum of eNOS lysate after BH_4 addition. Tetrahydrobiopterin addition caused a shift in the peak position of the $\mathbf{g}_x$ feature to 7.53, closely matching the effect of BH_4 on the arginine complex of the purified enzyme. This indicates that BH_4 is able to bind to the enzyme *in situ*, thus making it unnecessary to eliminate by purification endogenous pterins which could compete for the binding site. The EPR spectrum of NMA-treated lysate is shown in Figure 4, trace C. The $\mathbf{g}_x$ feature of the ferriheme has shifted from 7.60 to 7.73, in good agreement with results obtained with purified enzyme. Removal of endogenous substrate is not neccessary to observe inhibitor binding effects.

Conformational Stability during Extended Incubation. Eventual crystallization of eNOS and other NOS isoforms will require high-quality, high-concentration preparations which are stable for relatively long periods of time. Figure 5, trace A, shows the EPR spectrum at 10 K of a concentrated, high purity eNOS preparation which has been incubated for 3 weeks at 4 °C. The spectrum resembles that of freshly isolated eNOS, except that there is a much higher proportion of low-spin forms. We estimate the low-spin content to be approximately 80%, compared to 50−60% in isolated eNOS expressed in *E. coli* in the absence of BH_4. The EPR spectra of the low-spin region, with features near $\mathbf{g} = 2.41$, 2.28, and 1.9, are indicative of at least two low-spin components and are reminiscent of the spectra of nNOS heme domain preparations [$nNOS_{1-720}$ with His tags in its *N*-terminus, constructed as described by McMillan and Masters (1995); glutathione-S-transferase-$nNOS_{220-721}$ fusion protein as described in Masters *et al.* (1996)] in which the absence of the reductase domain apparently influences the stability of the high-spin states (J. C. Salerno, P. Martasek, K. McMillan, and B. S. S. Masters, unpublished observations).

As shown in trace B, addition of 100 μM NNA converts the preparation almost quantitatively to a single high-spin form with $\mathbf{g}_x = 7.3$, $\mathbf{g}_y = 4.47$, and $\mathbf{g}_z = 1.86$. The minor differences between this species and the species of Figure 2, trace C, are attributable to BH_4 effects on NOS high-spin ferriheme EPR spectra. The loss of the flavin free radical signal is due to slow auto oxidation. It is noteworthy that after 3 weeks of incubation, the low-spin states of the enzyme can be rescued by recruitment into a single, nearly homogeneous high-spin state by the addition of a strong arginine analog inhibitor. There is no detectable formation of axial $\mathbf{g} = 6$ high spin, indicative of loss of the thiolate ligand and roughly equivalent to the formation of heme sites which form ferrous CO complexes with 420 nm Soret bands. The result demonstrates that the eNOS holoenzyme heme binding region is stable during long incubation at 4 °C. The principal change in the heme environment can be attributed to the reversible binding of a sixth ligand trans to the thiolate. This happens much more rapidly in heme domain preparations.

DISCUSSION

Binding of ligands to the arginine site of eNOS perturbs both the spin state equilibrium and the ligation geometry of the ferriheme. Addition of substrate (L-arginine), intermediate (NHA), and L-arginine analog inhibitors produced ligand-specific high-spin ferriheme species, with characteristic spectroscopic signatures depending on the nature of the substituents presented to the heme pocket. The results presented here are qualitatively quite similar to our previous findings for nNOS, but the differences between the two isoforms are significant and shed light on the partial isoform specificity previously observed for some arginine analog inhibitors.

The high-spin ferriheme EPR spectra presented here are controlled by the ratio of the zero field splitting parameters, E and D. As E/D increases, $\mathbf{g}_x$ and $\mathbf{g}_y$ split about ~6 and lower both $\mathbf{g}_z$ and $(\mathbf{g}_x + \mathbf{g}_y)/2$ as a second-order effect. The system is well described by the $S = {}^5/_2$ spin Hamiltonian $D\{S_z^2 - 1/3[S(S+1)]\} + E(S_x^2 - S_y^2)$, and the features of the EPR spectra observed can be shown to result from E/D ratios in the range 0.058−0.088. The zero field splitting parameters reflect differential admixture by spin-orbit coupling of low-lying states into the ground state $^6A_1$ sextet due to tetragonal and rhombic splitting of the t_{2g} d orbitals. Changes in rhombicity reported here are dominated by differences in E which depend on the nature and orientation of the axial ligand.

As we have previously pointed out, changes in E/D in model complexes have been primarily attributed to changes in the character of the axial ligand; for example, to the acidity of the axial thiolate. This is not a good model for the changes observed upon substrate analog binding in proteins. It is more likely that the changes reflect distortion of the iron coordination sphere driven by interactions of arginine site ligands with the polypeptide (and possibly with the porphyrin). Readjustments within the heme pocket cause changes in the length and orientation of the thiolate−metal bond with respect to the porphyrin plane, which then affect E/D through the d orbital splittings. A better model for this kind of effect will eventually be provided when sufficient single crystal EPR data is available from soluble P450 enzymes.

Table 1 summarizes the characteristics of the eNOS ferriheme species obtained in experiments presented. The range of rhombicities covered by the high-spin species indicates that thiolate axial heme ligation is maintained in all cases, but that the geometry of the heme complex depends primarily on the ligand bound to the arginine site and to a lesser extent on the occupation of the pterin binding site. The rhombicity of the most prominent high-spin ferriheme component of eNOS as isolated appears to be similar to that of the L-arginine complex. This does not necessarily mean that L-arginine is bound to this fraction of the enzyme (20−25%); it is more likely that the most stable state of the enzyme with the arginine site empty is similar to the L-arginine complex. The empty state in nNOS resembles its NHA complex and eNOS, as isolated, has a high-spin component which resembles the eNOS L-arginine complex.

The L-arginine complex of eNOS is nearly completely high spin. The rhombicity of the L-arginine complex decreases on addition of BH_4, reflected in the decrease in the value of $\mathbf{g}_x$ from 7.58 to 7.53 (Figure 1). This suggests that the pterin binding site, as well as the arginine binding site, is coupled to heme ligation geometry. A similar shift was observed on addition of BH_4 to eNOS as isolated; the pterin-induced species was somewhat broader than the species seen in the presence of BH_4 and L-arginine but showed a similar reduction in rhombicity. This suggests that, while the effect of BH_4 is modulated by the occupancy of the arginine site, an effect of BH_4 binding on heme geometry is present which is either direct or (more likely) polypeptide mediated.

We recently classified the high-spin ferriheme complexes of nNOS (Salerno *et al*., 1996a). L-Arginine and arginine analogs produced four clusters of high-spin ferriheme states, which we attributed to the stabilization of local conformational states by ligand binding, producing a tendency to cluster around preexisting conformational energy minima. All the states represented five-coordinate thiolate axial ligation. Nearly pure states characteristic of each group were produced by the binding of L-arginine, NHA, NMA, and NNA, while some other ligands, e.g., thiocitrulline (Frey *et al*., 1994), produced equilibrium (as opposed to quantum mechanical) mixtures of states.

The arginine complexes of eNOS and nNOS are similar, but the eNOS complexes are consistently slightly lower in rhombicity. The $\mathbf{g}_x$ values of the well-defined BH_4−arginine complexes of nNOS and eNOS are, for example, 7.57 and 7.53, respectively. This subtle difference is reflected in other ferriheme complexes of eNOS, and represents an inherent difference in the active site. The NHA complex of eNOS is similar to the NHA complex of nNOS; again, the rhombicity is slightly smaller, reflected in $\mathbf{g}_x$ values for the NHA complexes of nNOS and eNOS of 7.68−7.69 and 7.67, respectively. It is possible that the lower rhombicity of the eNOS complexes is connected to the apparent bias toward the arginine-like state observed in the purified enzyme.

The lowest rhombicity complex is produced by NNA, which converts eNOS into a single state with $\mathbf{g}_x = 7.27$. A similar state (with $\mathbf{g}_x \approx 7.28$) was observed when nNOS was incubated with NNA. These complexes retain the axial thiolate ligand, but the large change in geometry produced by NNA binding suggests a significant rearrangement of the active site conformation. Both eNOS and nNOS form tight NNA complexes with long off-rate constants which may reflect the need for protein conformational change before ligand release.

N-Methyl arginine (NMA) is a more potent inhibitor of iNOS and nNOS than of eNOS. It has been reported to inactivate iNOS and nNOS irreversibly in a turnover-dependent manner. NMA is also a turnover-independent, competitive inhibitor of all three isoforms, but clearly is a less effective inhibitor of eNOS than of the other two isoforms (Reif & McCreedy, 1995).

NMA forms a turnover-independent complex with nNOS with a very low (sub micromolar) K_d; the rhombicity of this complex is the highest we have observed with nNOS holoenzyme. The NMA complex of eNOS is also higher in rhombicity than any other eNOS complex. However, comparison of the corresponding complexes of the isoforms reveals that the eNOS NMA complex is significantly less rhombic than the nNOS NMA complex; $\mathbf{g}_x$ is around 7.73 for eNOS and 7.77−7.78 for nNOS. All of the eNOS complexes (except for IEO) are at least slightly less rhombic than the corresponding complex of nNOS, but the difference is more pronounced in the case of NMA.

It is probable, although not yet proven, that the isoform "specificity" of NMA and the inability of eNOS to form an NMA complex of comparable rhombicity to iNOS and nNOS are related. The lower rhombicity of the eNOS NMA complex suggests that eNOS lacks the ability to assume the active site conformation associated with NMA binding in the other two isoforms. This may prevent the production of the putative irreversible inhibitor, or may result in a reduced affinity for inhibitors which bind in an NMA-like mode.

The bulky substituents of NMA and NNA present steric challenges to the arginine binding site, and NOS isoforms appear to respond to these challenges by employing very different active site conformations/binding modes. The three isoforms differ significantly in their ability to assume these states, which may reflect differences in flexibility and/or steric constraints. Greater understanding of the relationships between the active sites can be obtained by comparative studies using a wider range of arginine analogs.

Effects of BH_4 and L-Arginine on the Flavin Radical. It is clear from the results presented here that L-arginine and BH_4 diminish the flavin radical present in the enzyme as isolated. By analogy with the homologous NADPH-cytochrome P450 reductase (CPR), the radical probably corresponds to the FMNH flavosemiquinone. Loss of the radical signal could result from semiquinone oxidation, semiquinone reduction, or semiquinone disproportionation. The processes leading to the loss of the radical are slow and may have no catalytic significance. By analogy with CPR, we expect the semiquinone state of FMN to be the most oxidized redox partner in the physiological state and to be too poor a reductant to support catalytically significant turnover. Valuable lessons may, however, eventually emerge from consideration of these phenomena.

Arginine/BH_4-driven conformational perturbations could destabilize the radical with respect to ferroheme and contribute to its loss. This is consistent with NOS being "primed" for heme reduction by interaction with its substrate, L-arginine. The decrease in free radical caused by arginine addition could also be explained by a slow single turnover of the enzyme at the expense of L-arginine. Production of small amounts of NHA and citrulline has been reported previously (Campos *et al.*, 1995). It is of interest that

overnight incubation with BH_4 and L-arginine produced a ferriheme with the characteristics of the L-arginine complex in the absence of BH_4, although this might have resulted from nonenzymatic BH_4 oxidation. Loss of radical signal after addition of BH_4 alone is not so easily explained in terms of flavin oxidation. Arginine analog inhibitors protected the radical against BH_4, suggesting that the heme site is involved in radical loss. The apparent restoration of the radical in some cases might result from slow electron transfer from BH_4 to flavin, allowing radical to build up after the pathway destroying it is inhibited.

The experiments reported in this study constitute a comprehensive examination of substrate, intermediate, and substrate analog inhibitors as probes of the heme pocket of the three isoforms of nitric oxide synthase expressed in and purified from stably transfected human kidney embryonic cells or from *E. coli* in the Masters' laboratory. First, utilization of optical difference spectroscopy (McMillan & Masters, 1993; Frey *et al*., 1994) and, later, of EPR spectroscopy (Salerno *et al*., 1995, 1996a,b) has permitted the classification of interactions among these substrate/intermediate/inhibitors. The perturbation of the heme environment by substrate analogs, reflected in the formation of high-spin complexes of distinct geometry, could then be related to their effectiveness as substrate/inhibitors relative to each NOS isoform. It is now possible to "map" the active sites of the various isoforms through examination of a variety of substrate analogs. Results from these experiments should provide insight into isoform-specific inhibitor design in the absence of three-dimensional structure data.

REFERENCES

Abu-Soud, H. M., & Stuehr, D. J. (1993) *Proc. Natl. Acad. Sci. U.S.A. 90*, 10769−10772.

Bredt, D. S., Hwang, P. M., Glatt, C. E., Lowenstein, C., Reed, R. R., & Snyder, S. H. (1991) *Nature 351*, 714−718.

Bredt, D. S., Ferris, C. D., & Snyder, S. H. (1992) *J. Biol. Chem. 267*, 10976−10981.

Bromberg, Y., & Pick, E. (1989) *Cell. Immunol. 52*, 73−83.

Campos, K. L., Giovanelli, J., & Kaufman, S. (1995) *J. Biol. Chem. 270*, 1721−1728.

Chen, P. F., Tsai, A. L., Berka, V., & Wu K. K. (1996) *J. Biol. Chem. 271*, 14631−14635..

Cho, H. J., Xie, Q., Calaycay, J., Mumford, R. E., Swiderek, K. M., Lee, T. D., & Nathan, C. (1992) *J. Exp. Med. 176*, 599−604.

Curran, R. D., Billiar, T. R., Stuehr, D. J., Hofmann, K., & Simmons, R. L. (1989) *J. Exp. Med. 170*, 1769−1774.

Frey, C., Narayanan, K., McMillan, K., Spack, L., Gross, S. S., Masters, B. S. S., & Griffith, O. W., (1994) *J. Biol. Chem. 269*, 26083−26091.

Furchgott, R. F. (1988) in *Vasodilatation: Vascular Smooth Muscle, Peptides, Autonomic Nerves, and Endothelium* (Vanhoutte, P. M., Ed.) pp 401−414, Raven Press, New York.

Gachhui, R., Presta, A., Bentley, D. F., Abu-Soud, H. M., McArthur, R., Brudwig, G., Ghosh, D. K., & Stuehr, D. J. (1996) *J. Biol. Chem. 271*, 20594−20602.

Garthwaite, J., Charles, S. L., & Chess-Williams, R. (1988) *Nature 336*, 385−388.

Ghosh, D. K., & Stuehr, D. J. (1995) *Biochemistry 34*, 801−807.

Hauschildt, S., Lucknoff, A., Mulsch, A., Kohler, J., Bessler, W., & Buse, R. (1990) *Biochem. J. 270*, 351−356.

Hibbs, J. B., Jr., Taintor, R. R., & Vavrin, Z. (1987) *Science 235*, 473−476.

Ignarro, L. J., Buga, G. M., Wood, K. S., Byrns, R. E., & Chaudhuri, G. (1987) *Proc. Natl. Acad Sci. U.S.A. 84*, 9265−9269..

Iyengar, R., Stuehr, D. J., & Marletta, M. A. (1987) *Proc. Nat. Acad. Sci. U.S.A. 84*, 6369−6373.

Jaussens, S. P., Shimouchi, A., Quertermous, T., Bloch, D. B., & Bloch, K. D. (1992) *J. Biol. Chem. 267*, 14519−14522.

Knowles, R. G., Palacios, M., Palmer, R. M. J., & Moncada, S. (1990) *Biochem. J. 269*, 207−210.

Lamas, S., Marsden, P. A., Li, G. K., Tempst, P., & Michel, T. (1992) *Proc. Natl. Acad. Sci. U.S.A. 89*, 6348−6352.

Lyons, C. R., Orloff, G. J., & Cunningham, J. M. (1992) *J. Biol. Chem. 267*, 6370−6374.

Marletta, M. A., Yoon, P. Y., Iyengar, R., Leaf, C. D., & Wishnok, J. S. (1988) *Biochemistry 27*, 8706−8711.

Martásek, P., Liu, Q., Liu, J., Roman, L. J., Gross, S. S., Sessa, W. C., & Masters, B. S. S. (1996) *Biochem. Biophys. Res. Commun. 219*, 359−365.

Masters, B. S. S., McMillan, K., Roman, L. R., Martasek, P., & Nishimura, J. (1996) *Methods Neurosci. 31*, 140−151.

Mayer, B., John, M., Heinzel, B., Werner, E. R., & Wachter, H. (1991) *FEBS Lett. 288*, 187−191.

McCall, T. B., Boughton-Smith, N. K., Palmer, R. M. J., Whittle, B. J. R., & Moncada, S. (1989) *Biochem. J. 262*, 293−296.

McMillan, K., Bredt, D. S., Hirsch, D. J., Snyder, S. H., Clark, J. E., & Masters, B. S. S. (1992) *Proc Nat. Acad. Sci. U.S.A. 89*, 11141−11145.

McMillan, K., & Masters, B. S. S. (1995) *Biochemistry 34*, 3686−3693.

Nishimura, J. S., Martasek, P., McMillan, K., Salerno, J. C., Liu, Q., Gross, S. S., & Masters, B. S. S. (1995) *Biochem. Biophys. Res. Commun. 210*, 288−294.

Palmer, R. M. J., Ferrige, D. S., & Moncada, S. (1987) *Nature 327*, 524−526.

Palmer, R. M. J., Ashton, A. G., & Moncada, S. (1988) *Nature 333*, 664−666.

Reif, D. W., & McCreedy, S. A. (1995) *Arch. Biochem. Biophys. 320*, 170−176.

Salerno, J. C., Frey, C., McMillan, K., Williams, R., Masters, B. S. S., & Griffith, O. W. (1995) *J. Biol. Chem. 270*, 27423−27428.

Salerno, J. C., McMillan, K., & Masters, B. S. S. (1996a) *Biochemistry 35*, 11839−11845.

Salerno, J. C., Martasek, P., Roman, L. J., & Masters, B. S. S. (1996b) *Biochemistry 35*, 7626−7630.

Stuehr, D. J., & Ikeda-Saito, M. (1992) *J. Biol. Chem. 267*, 20547−20550.

White, K. A., & Marletta, M. A. (1992) *Biochemistry 31*, 6627−6631.

Xie, Q., Cho, H. J., Calacay, J., Mumford, R. A., Swiderek, K. M., Lee, T. D., Ding, A., Troso, T., & Nathan, C. (1992) *Science 256*, 225−228.

BI963003Q